

# Effective Photon Spectra for the Photon Colliders

I.F. Ginzburg

Institute of Mathematics, Prosp. Acad. Koptyug 4, 630090 Novosibirsk, Russia,  
e-mail: ginzburg@math.nsc.ru,

G.L. Kotkin

Novosibirsk State University, Ul. Pirogova 2, 630090 Novosibirsk, Russia,  
e-mail: kotkin@math.nsc.ru

## Abstract

The luminosity distribution in the effective  $\gamma\gamma$  mass at a photon collider has usually two peaks which are well separated: the High energy peak with mean energy spread about 5 – 7% and the wide low energy peak. The low energy peak depends strongly on details of design and is unsuitable for the study of New Physics phenomena. We find simple approximate form of spectra of *colliding photons* for  $\gamma\gamma$  and  $e\gamma$  colliders, whose convolution describes high energy luminosity peak with good accuracy in the most essential preferable region of parameters.

## 1 Introduction

The photon colliders ( $\gamma\gamma$  and  $e\gamma$ ) were proposed and discussed in details in Refs. [1]. The forthcoming papers [2, 3] present some new details of design and analysis of some effects involved in conversion.

In a basic scheme two electron beams leave the final focus system and travel towards the interaction point (IP). At the conversion point (CP) at the distance  $b \sim 1 - 10$  mm before IP they collide with focused laser beams. The Compton scattering of a laser photon on an electron produces a high energy photon. The longitudinal motion of this photon originates from that of an electron, so that these photons follow the trajectories of electrons (to the IP) with additional angular spread  $\sim 1/\gamma$ . With reasonable laser parameters, one can "convert" most of the electrons into the high energy photons. Without taking into account rescattering of electrons on the next laser photons, the total  $\gamma\gamma$  and  $e\gamma$  luminosities are  $\mathcal{L}_{\gamma\gamma}^0 = k^2 \mathcal{L}_{ee}$  and  $\mathcal{L}_{e\gamma}^0 = k \mathcal{L}_{ee}$  where  $k$  is the conversion coefficient and  $\mathcal{L}_{ee}$  is the geometrical luminosity of basic  $ee$  collisions, which can be made much larger than the luminosity of the basic  $e^+e^-$  collider. Below we assume distances  $b$  and the form of the electron beams to be identical for both beams.

Let the energy of the initial electron, laser photon and high energy photon be  $E$ ,  $\omega_0$  and  $\omega$ . We define as usual

$$x = \frac{4E\omega_0}{m_e^2}, \quad y = \frac{\omega}{E} \leq y_m = \frac{x}{x+1}. \quad (1)$$

The quality of the photon spectra is better for higher  $x$ . However at  $x > 2(1 + \sqrt{2}) \approx 4.8$  the high energy photons can disappear via production of  $e^+e^-$  pair in its collision with a following laser photon. That is why the preferable conversion is at  $x = 4 - 5$ .

The energies of colliding photons  $\omega_i = y_i E$  can be determined for each event by measuring the total energy of the produced system  $\omega_1 + \omega_2$  and its total (longitudinal) momentum  $\omega_1 - \omega_2$ . We discuss in more detail the main area for study of New Physics — **the high energy region** where energies of both photons are large enough. For the definiteness we consider the photon energy region  $(y_m/2) < y_i < y_m$  and demand additionally that no photons with lower energy contribute to the entire distribution over the effective mass of  $\gamma\gamma$  system  $2zE$  or its total energy  $YE$ :

$$\frac{y_m}{2} < y_1, y_2 < y_m \Rightarrow \left( \frac{y_m}{\sqrt{2}} < z = \sqrt{y_1 y_2} < y_m \right), \quad (1.5y_m < Y = y_1 + y_2 < 2y_m). \quad (2)$$

In the interesting cases this choice covers the high energy peak in luminosity since the photon spectra are concentrated in the more narrow regions near  $y_m$ .

The growth of the distance  $b$  between IP and CP is accompanied by two phenomena. First, high energy collisions become more monochromatic. The high energy part of luminosity is concentrated in a relatively narrow peak which is separated well from an additional low energy peak. This separation becomes stronger at higher  $x$  and  $b$  values. Second, the luminosity in the high energy region decreases (relatively slowly at small  $b$  and as  $b^{-2}$  at large  $b$ ). Only the high energy peak is the area for study of the New Physics phenomena. The low energy peak is the source of background at these studies. The separation between peaks is very useful to eliminate background from the data. Therefore, some intermediate value of  $b$  provides the best conditions for study of New Physics.

Let us discuss spectra neglecting rescattering, for beginning. At  $b = 0$  the  $\gamma\gamma$  luminosity distribution is a simple convolution of two photon spectra of separate photons. At  $b \neq 0$  the luminosity distribution is a more complicated convolution of the above photon spectra with some factor depending on  $b$  and the form of initial electron beams. With the growth of conversion coefficient the effect of rescattering of electrons on laser photons enhances and make this distribution dependent on the details of design (mainly, in low energy part).

In this paper we continue the discussion from Ref. [1] about main parameters of scheme which are preferable for the  $\gamma\gamma$  and  $e\gamma$  colliders for the elliptic electron beams. We find the universal description of high energy peak in this preferable region of parameters. It allows us to obtain the remarkable approximate form of spectra of **colliding photons**, whose simple convolution describes high energy luminosity peak with reasonable accuracy.

## 2 Luminosity distribution without rescattering. Elliptic electron beams

The high energy peak in luminosity is described mainly by a single collision of an electron with a laser photon, this part of distribution depends on the form of initial beams only. Therefore we start with the detailed discussion of effects from single electron and laser photon collision. At first, we repeat some basic points from Refs. [1].

The scattering angle of produced photon  $\theta$  is related to its energy as

$$\theta = \frac{g(x, y)}{\gamma}, \quad g(x, y) = \sqrt{\frac{x}{y} - x - 1}, \quad \gamma = \frac{m_e}{E}. \quad (3)$$

Let the mean helicities of initial electron, laser photon and high energy photon be  $\lambda_e/2$ ,  $P_\ell$  and  $\xi_2$ . The energy spectrum of produced photons is ( $N$  is normalization factor)

$$F(x, y) = N \left[ \frac{1}{1-y} - y + (2r-1)^2 - \lambda_e P_\ell x r (2r-1)(2-y) \right], \quad r = \frac{y}{x(1-y)}. \quad (4)$$

At  $\lambda_e P_\ell = -1$  and  $x > 1$  this spectrum has a sharp peak at high energy which becomes even more sharp with  $x$  growth.

The spectrum is more sharp when  $-\lambda_e P_\ell$  is larger. We present below mainly the values from the real projects  $\lambda_e = 0.85$ ,  $P_\ell = -1$ .

The degree of circular polarization of high energy photon is

$$\langle \xi_2 \rangle = N \frac{\lambda_e x r \left[ 1 + (1-y)(2r-1)^2 \right] - P_\ell (2r-1) \left[ \frac{1}{1-y} + 1-y \right]}{F(x, y)}. \quad (5)$$

The photons with lower energy have higher production angle (3). With the growth of  $b$ , these photons spread more and more, and they collide only rarely. Therefore, with the growth of  $b$  photon collisions become more monochromatic, only high energy photons taking part in these collisions the low energy part of total luminosity being rejected (here photons in the average are almost nonpolarized).

This effect was studied in [1] for the gaussian round electron bunches. However, the incident electron beams are expected to be of an elliptic form with large enough ellipticity.

Let initial electron beams be of the gaussian elliptic form with vertical and horizontal sizes  $\sigma_{ye}$  and  $\sigma_{xe}$  at the IP (calculated for the case without conversion). The discussed phenomena are described by a reduced distance between conversion and collision points  $\rho$  and an aspect ratio  $A$

$$\rho^2 = \left( \frac{b}{\gamma \sigma_{xe}} \right)^2 + \left( \frac{b}{\gamma \sigma_{ye}} \right)^2, \quad A = \frac{\sigma_{xe}}{\sigma_{ye}}. \quad (6)$$

The luminosity distributions in this case can be calculated by the same approach which was used in Ref. [1].

The distribution of the photons colliding with opposite electrons at  **$e\gamma$  collider** is

$$\frac{d\mathcal{L}_{e\gamma}}{dy} = \int \frac{d\phi}{2\pi} F(x, y) \exp \left[ -\frac{\rho^2 g^2(x, y)}{4(1+A^2)} (A^2 \cos^2 \phi + \sin^2 \phi) \right]. \quad (7)$$

For the round beams ( $A = 1$ ) we have in the exponent  $\rho^2 g^2(x, y)/8$ .

The distribution of the colliding photons over their energies at  **$\gamma\gamma$  collider** is

$$\frac{d^2 \mathcal{L}_{\gamma\gamma}}{dy_1 dy_2} = \int \frac{d\phi_1 d\phi_2}{(2\pi)^2} F(x, y_1) F(x, y_2) \exp \left[ -\frac{\rho^2 \Psi}{4(1+A^2)} \right], \quad (8)$$

$$\Psi = A^2 [g(x, y_1) \cos \phi_1 + g(x, y_2) \cos \phi_2]^2 + [g(x, y_1) \sin \phi_1 + g(x, y_2) \sin \phi_2]^2.$$

For the round beams ( $A = 1$ ) one can perform integrations over  $\phi_i$  in the analytical form. It results in the equation from Ref. [1] with the Bessel function of an imaginary argument  $I_0(v^2)$

$$\frac{d^2 \mathcal{L}_{\gamma\gamma}}{dy_1 dy_2} = F(x, y_1) F(x, y_2) \exp \left[ -\frac{\rho^2}{8} (g^2(x, y_1) + g^2(x, y_2)) \right] I_0(v), \quad (9)$$

$$v^2 = \frac{\rho^2}{4} g(x, y_1) g(x, y_2).$$

We have analyzed numerically the high energy part of the luminosity (in the region (2))  $\mathcal{L}^h$  as a function of  $\rho^2$  and  $A$  at  $2 < x < 5$ ,  $-\lambda_e P_\ell \geq 0$ . (We use this notation for both total luminosity integrated over the region (2) and differential distributions.)

The growth of  $\rho$  results both in a better form of luminosity distribution and reduction of luminosity. We find that the luminosity  $\mathcal{L}^h$  depends only weakly on the aspect ratio  $A$  at  $A > 1.5$  and  $\rho^2 < 1.3$ . At  $\rho^2 \leq 1$  this dependence is weak at all values of  $A$  (including  $A = 1$ ). For  $\lambda_e P_\ell = -0.85$  the luminosity  $\mathcal{L}^h$  at  $\rho = 1$  contains large enough fraction from the high energy part of luminosity given at  $\rho = 0$ . For the unpolarized case ( $\lambda_e P_\ell = 0$ ) both this fraction is smaller and the high energy peak is separated weakly from the low energy one. Some of these statements can be seen from the table below where we show the ratio of high energy luminosity  $\mathcal{L}^h$  to the total luminosity  $\mathcal{L}_{\gamma\gamma}^0$  at some values of parameters.

	$\rho = 0$ , any $A$		$\rho = 1$ , $A \geq 1.5$	
$\lambda_e P_\ell$	-0.85	0	-0.85	0
$x = 4.8$	0.35	0.25	0.28	0.19
$x = 2$	0.29	0.19	0.25	0.16

It seems unreasonable to use lowest part of total luminosity than that obtained at  $\rho = 1$ .

To have a more detailed picture for the simulation, we study the luminosity distribution in the relative values of the effective mass  $z = W/(2E)$  and the total energy  $Y = \mathcal{E}/E$  of the pair of colliding photons (2). Their typical forms for different values of aspect ratio  $A$  are shown in Figs. 1, 2.

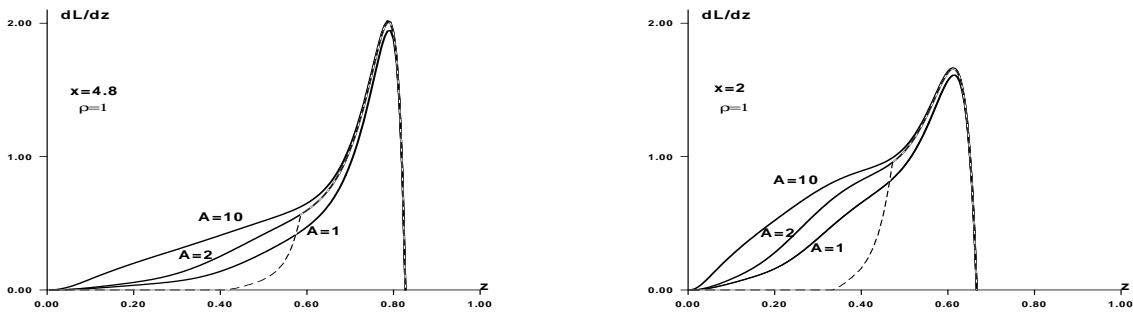


Figure 1: The luminosity distributions in the effective mass of  $\gamma\gamma$  system at  $\lambda_e P_\ell = -0.85$ . Dashed line presents this distribution for  $y_i > y_m/2$  at  $A = 2$ .

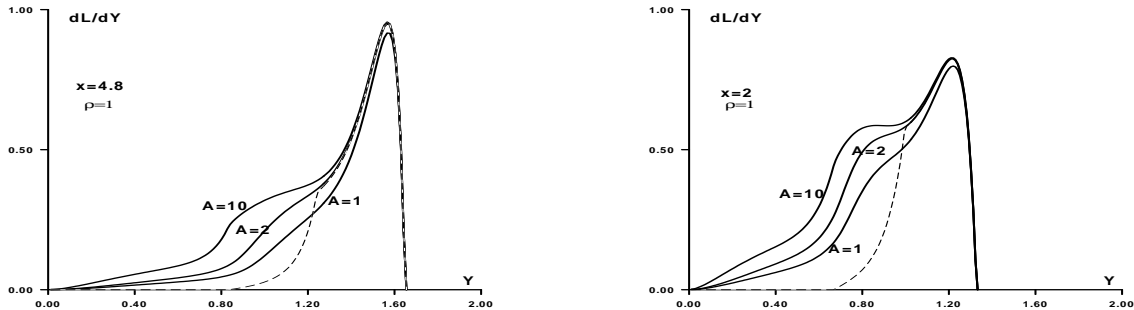


Figure 2: *The luminosity distributions in the total energy of  $\gamma\gamma$  system at  $\lambda_e P_\ell = -0.85$ . Dashed line presents this distribution for  $y_i > y_m/2$  at  $A = 2$ .*

The numerical study of these distributions shows us that its high energy part is practically the same for all values  $A > 1.5$  at fixed  $\rho^2 < 1.3$  (with small difference near lower part of peak). The luminosity within high energy peak for round beams ( $A = 1$ ) is slightly lower than that for the elliptic beams. This difference is about 5% in the main part of region below peak. At  $\rho^2 = 1$  this difference is small for all  $A$ . At  $\rho^2 > 0.5$  the high energy part of luminosity has the form of a narrow enough peak. This peak is not so sharp at lower  $x$  and it is even less sharp at  $\lambda_e P_\ell = 0$ .

With the growth of aspect ratio  $A$  the entire distributions acquire low energy tails (as compared with round beams) originated from the collisions of low energy photons scattered near the horizontal direction with the opposite high energy photon scattered in the vertical direction. This tail is added to that from the rescatterings and is not of much interest in the discussion of high energy peak. At higher  $\rho$  and  $A$  this effect becomes more essential in the region of the peak.

As a result, the preferable region of parameters for photon colliders is

$$5 > x > 2, \quad -\lambda_e P_\ell \geq 0.5, \quad \rho^2 < 1.3. \quad (10)$$

Additionally, here the high energy peaks in the  $\gamma\gamma$  and  $e\gamma$  luminosities are described by one parameter  $\rho$  and practically independent from  $A > 1.5$ .

### 3 Rescattering contribution to the spectra. Qualitative description

The rescattering of electrons on the following laser photons produces new high energy photons (*secondary photons*) which modify the luminosity distribution mainly in the low energy part. Detailed form of additional components of luminosity distribution depends strongly on the conversion coefficient and other details of design. That is why we present here only qualitative discussion with some simple examples.

Let us enumerate the differences in properties of secondary photons from those from the first collision (we will denote them as *primary photons*).

- (1) The energy of secondary photons is lower than that of primary photons.
- (2) There is no definite relation between energy and production angle like (3).
- (3) The mean polarization of secondary photons is practically zero.

Fig. 3 presents a typical energy spectrum of photons with only one rescattering at conversion coefficient  $k = 1$ . Dashed line represents fraction of secondary photons. Let us explain some features of this spectrum.

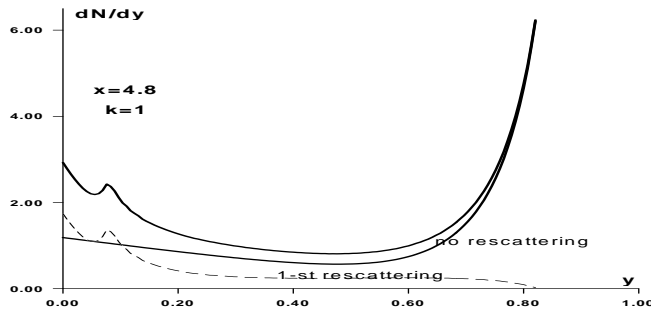


Figure 3: *The energy spectrum of photons with one rescattering,  $\lambda_e P_\ell = -0.85$ .*

The main fraction of electrons after the first scattering has the energy which corresponds to the peak in produced photons spectra,  $E_e \approx E - \omega_m = E/(x + 1)$ . For the next collision  $x \rightarrow x/(x + 1)$ . Therefore, the additional energy peak in photon spectrum caused by secondary photons from the first rescattering is at the photon energy  $\sim y_m/(2x + 1)$ , it is much lower than  $y_m E$  for  $x > 2$ . The subsequent rescatterings add more soft photons. Besides, the primary photon spectrum (4) is concentrated near its high energy boundary. So, the fraction of scattered electrons with energy close to  $E$  is small, the effect of rescattering in a high energy part on the entire photon spectrum is also small. In the subsequent rescatterings such peaks become smooth. The well known result is a large peak near  $y = 0$ . Note also that the secondary photons in average are nonpolarized.

The shape of an additional contribution of secondary photons to the luminosity distributions (second–second and primary–second) depends on  $k$ ,  $\rho$  and  $A$ . Nevertheless, the different simulations show the common features (see [2, 3]):

At  $\rho^2 \geq 0.5$ ,  $k \lesssim 1$  the luminosity distribution has two well separated peaks: **high energy peak (mainly from primary photons) and wide low energy peak (mainly from secondary photons)**. Photons in the high energy peak have high degree of polarization, mean polarization of photons in the low energy peak is close to 0. At smaller  $x$  or  $-\lambda_e P_\ell$  this separation of peaks becomes less definite and mean photon polarization becomes less than that given by Eq. (5).

With a good separation of peaks, the backgrounds from the low energy peak could be eliminated relatively easily in many problems.

## 4 Approximation

The previous discussion shows us that there are chances to construct an approximation for photon spectra which would describe the high energy peak simply and in the universal way. We were searching for an approximation in which the high energy peak in  $\gamma\gamma$  luminosity would be given by a simple convolution of form

$$\frac{d^2\mathcal{L}}{dy_1 dy_2} = F_a(x, y_1, \rho^2) F_a(x, y_2, \rho^2). \quad (11)$$

instead of complex integration (8) (independent from aspect ratio  $A$ ).

We tested different forms of effective photon spectra. Taking into account form of angular spread of separate beam, we consider a test function for the high energy peak in the form

$$F_a(x, y, \rho^2) = \begin{cases} F(x, y) \exp[-B\rho^2 g(x, y)^2/8] & \text{at } y > y_m/2, \\ 0 & \text{at } y < y_m/2. \end{cases} \quad (12)$$

where coefficient  $B$  is varied.

A good fit for the high energy peak at  $2 < x < 5$ ,  $\rho^2 < 1.3$ ,  $A > 1.5$  is given by the values

$$\begin{aligned} B = 1 & \quad \text{for the } \gamma\gamma \text{ collider,} \\ B = 0.7 & \quad \text{for } e\gamma \text{ collider.} \end{aligned} \quad (13)$$

The curves in Figs. 4,5 show the accuracy of this approximation for the distributions in both the effective  $\gamma\gamma$  mass  $z = \sqrt{y_1 y_2}$  and the total photon energy  $Y = y_1 + y_2$  at  $\lambda_e P_\ell = -0.85$ . These curves show the excellent quality of our approximation. The distributions calculated without angular spread factor (at  $B = 0$ ) are also shown here by dashed lines. These curves are markedly higher than the precise curve and they are wider than the real distributions. The first inaccuracy can be compensated by a suitable renormalization, but the second inaccuracy cannot be eliminated from calculations.

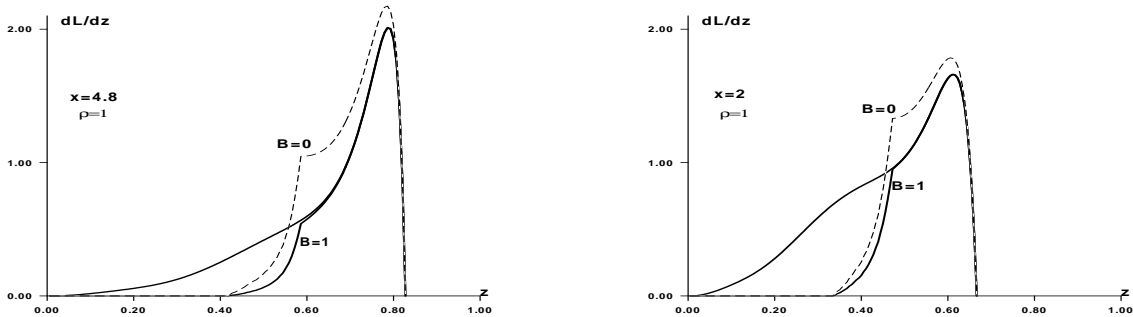


Figure 4: The precise luminosity distribution in the effective mass of  $\gamma\gamma$  system without rescattering at  $A = 2$  and approximation (11) – (13). Dashed line – approximation used spectra at  $\rho = 0$  in the region (2).

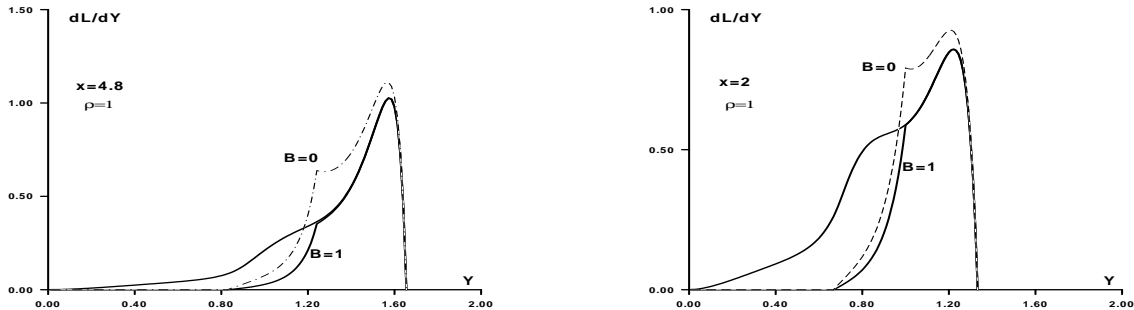


Figure 5: *The precise luminosity distribution in the total energy of  $\gamma\gamma$  system without rescattering at  $A = 2$  and approximation (11) – (13). Dashed line – approximation used spectra at  $\rho = 0$  in the region (2).*

Note that the approximation (13) for the  $\gamma\gamma$  collision can be obtained from eq. (9) if Bessel function  $I_0(v^2)$  are replaced by unity. Figs. 4,5 show that our approximation coincide practically with precise distributions within high energy peak for the elliptic beams ( $A \geq 1.5$ ). Therefore, the difference between curves for  $A = 1$  and  $A = 2$  in Figs. 1,2 in the region (2) is caused by the Bessel function factor.

Using of "precise" Eq. (8) instead of our approximation is only a sham improvement. The difference between the approximation and the "precise" formula is usually smaller than the effect of rescatterings.

## 5 Results

Let us enumerate the main results.

- The variable  $\rho$  (6) is a good variable for the description of the high energy peak in the spectral luminosity independent from the aspect ratio  $A$  at  $A > 1.5$ ,  $\rho^2 < 1.3$ ,  $2 < x < 5$ ,  $\lambda_e P_\ell < 0$ .
- At  $\rho \sim 1$  and suitable polarizations of initial beams the high energy peak in luminosity is separated well from the low energy peak. This separation can be destroyed by using of large conversion coefficient or (and) values  $x \approx 1$  or  $\lambda_e P_\ell > 0$ .
- To discuss future experiments at photon collider with good enough accuracy, one can use simple approximation (11)– (13) at  $\rho = 1$  instead of details simulation of conversion and collision. In this approximation the details of design are inessential. Possible decreasing of  $\rho^2$  to the value 0.5 can be also considered.
- The numbers describing luminosity of Photon Collider correspond the discussed high energy peak only.



## Acknowledgments

We are grateful to G. Jikia, V.G. Serbo and V.I. Telnov for the useful discussions. This work was supported by grant RFBR 99-02-17211 and grant of Sankt–Petersburg Center of Fundamental Sciences.

## References

- [1] I.F. Ginzburg, G.L. Kotkin, V.G. Serbo, V.I. Telnov, Nucl. Instr. Methods (NIM) **205** (1983) 47; I.F. Ginzburg, G.L. Kotkin, S.L. Panfil, V.G. Serbo, V.I. Telnov, NIM **219** (1984) 5.
- [2] See e.g. *Proc. Workshop on  $\gamma\gamma$  Colliders*. NIM **A355** 1-194. Zeroth-order Design Report for the NLC, SLAC Report 474 (1996); TESLA, SBLC Conceptual Design Report, DESY 97-048, ECFA-97-182 (1997); R.Brinkmann et. al., NIMR **A406** (1998) 13; I. Watanabe et al. KEK Report 97-17.
- [3] V.I. Telnov, hep-ex/9810019 and references therein.